

# A Mask-Based Adversarial Defense Scheme

Weizhen Xu, Chenyi Zhang, Fangzhen Zhao and Liangda Fang  
Jinan University

## Abstract

Adversarial attacks hamper the functionality and accuracy of Deep Neural Networks (DNNs) by meddling with subtle perturbations to their inputs. In this work, we propose a new Mask-based Adversarial Defense scheme (MAD) for DNNs to mitigate the negative effect from adversarial attacks. To be precise, our method promotes the robustness of a DNN by randomly masking a portion of potential adversarial images, and as a result, the output of the DNN becomes more tolerant to minor input perturbations. Compared with existing adversarial defense techniques, our method does not need any additional denoising structure, nor any change to a DNN’s design. We have tested this approach on a collection of DNN models for a variety of data sets, and the experimental results confirm that the proposed method can effectively improve the defense abilities of the DNNs against all of the tested adversarial attack methods. In certain scenarios, the DNN models trained with MAD have improved classification accuracy by as much as 90% compared to the original models that are given adversarial inputs.

## 1 Introduction

Deep Neural Networks (DNNs) have achieved great success in the past decade in research areas such as image classification, natural language processing, and data analytics, with a variety of application domains like banking, financial services and insurance, IT & Telecom, manufacturing, and healthcare etc., [Report, 2020]. However, researchers have discovered that it is possible to introduce human imperceptible perturbations to inputs of a DNN in a certain way that induces incorrect or misleading outputs from the DNN at the choice of an adversary [Szegedy *et al.*, 2014; Goodfellow *et al.*, 2015; Papernot *et al.*, 2016a]. As of today, the bulk of the existing defense approaches can be roughly grouped in two categories, i.e., they either focus on the detection of adversarial inputs (e.g., [Ma *et al.*, 2018; Cohen *et al.*, 2020; Xu *et al.*, 2018]), or to take steps to strengthen DNNs (e.g., [Meng and Chen, 2017; Madry *et al.*, 2018;

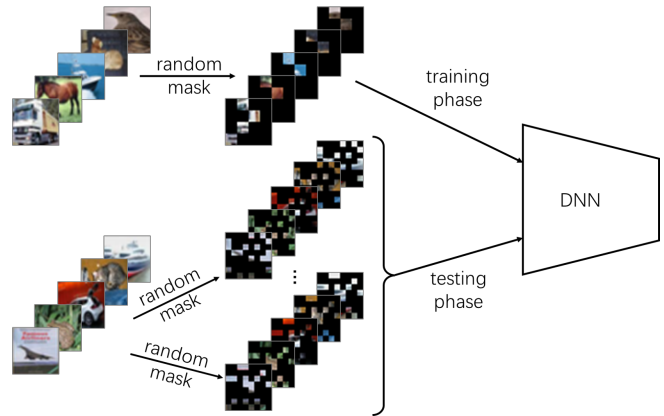


Figure 1: An overview of the MAD scheme

Mustafa *et al.*, 2019]), making them more robust to withstand perturbations on inputs.

In this paper, we follow the latter path by enhancing robustness in the decision procedure of DNNs. Again, there exist a rich class of works in the school of adversarial defense. Some early works propose adversarial training which applies adversarial inputs together with clean inputs at the time of training, in order to reduce the effectiveness of adversarial samples on DNNs [Madry *et al.*, 2018; Lee *et al.*, 2020], or distillation [Papernot *et al.*, 2016b] which trains a model to reduce the magnitude of gradients against adversarial attacks. Other approaches boost robustness of DNNs by redesigning training methods [Mustafa *et al.*, 2019], or apply filtering mechanisms that “correct” the adversarial inputs through autoencoder-based structures [Meng and Chen, 2017; Salman *et al.*, 2020]. Motivated by a recent paper [He *et al.*, 2021] which restores missing pixels of an image, we devise a new adversarial defense scheme called a Mask-based Adversarial Defense training method (MAD) for DNNs that classify images. In addition, we believe that such a mechanism may also be applicable to improve DNN robustness in other scenarios. Firstly, we have the following observations.

- Information density is often low in images, as missing patches from an image can often be mostly recovered by a neural network structure [He *et al.*, 2021] or by a human brain (as you look at something through a fence).

- Adversarial attacks on images usually introduce a minor perturbation to inputs, which may be reduced or cancelled by (randomly) covering part of the image.

In this approach, we split an image into grids of pre-defined size (e.g.,  $4 \times 4$ ), and randomly mask each grid with a given probability (e.g., 75%) into a default value (e.g., the black value in RGB for those masked pixels) to generate training samples. After the training, we also apply masking to images at the test stage (for the classification task), as illustrated in Fig. 1. Given an (unmasked) image, the test process is to be repeated a number of times, which makes a better chance of filtering out malicious perturbations, and the final decision is then defined as the mostly voted class taking into account the outputs for all randomly masked inputs.

**Contribution.** In this work, we introduce a new adversarial defence method MAD which applies masking at both the training phase and the test phase. This approach enjoys the following properties.

- Our method seems easily applicable to many existing DNNs. Compared with other adversarial defense methods, we do not need special treatment to the structures of DNNs, redesign of loss functions, or any (autoencoder-based) input filtering.
- The randomized masking at both the training phase and the test phase yields our method more resistant to adaptive white-box adversarial attacks.
- The experiment on a variety of models (LeNet, VGG and ResNet) has shown the effectiveness of our methods with a significant improvement in defense (up to 93% precision gain) when facing various adversarial samples, compared to the models without MAD.

## 2 Related Work

Since we work on an adversarial defense scheme, we conduct a brief overview to the mechanism of adversarial attacks and various types of adversarial defense works.

### 2.1 Adversarial attack

In general, an adversarial attack method generates tiny perturbations that are applied to clean inputs, making them incorrectly classified by a DNN. Some of the earliest methods include box-constrained L-BFGS [Szegedy *et al.*, 2014], Fast gradient sign method (FGSM) [Goodfellow *et al.*, 2015] and Jacobian-based Saliency Map Attack (JSMA) [Papernot *et al.*, 2016b]. Perhaps the most widely used attack method is FGSM, which is also included in our experiment. FGSM generates a perturbation for an image by computing the following.

$$\delta = \epsilon \operatorname{sign}(\nabla_x L(\theta, x, y)) \quad (1)$$

where  $L(\cdot)$  is the loss function used for neural network training which calculates the difference between label  $y$  and the output produced from input  $x$  for the DNN with parameter  $\theta$ . The direction of movement is obtained by the gradient of loss and constant  $\epsilon$  which restricts the norm of perturbation. Basic iterative method (BIM) [Kurakin *et al.*, 2017] and projected gradient descent (PGD) [Madry *et al.*, 2018] are the iteration

and extension of FGSM to obtain better attack effect, respectively.

The other advanced adversarial attack methods used in our experiments are DeepFool [Moosavi-Dezfooli *et al.*, 2016] and CW [Carlini and Wagner, 2017]. DeepFool computes an approximation of a minimal perturbation according to the DNN model’s decision boundary. In detail, given an image, DeepFool iteratively computes a small perturbation, taking into account the linearized boundary of region that contains the current perturbed image, thus it can be shown that DeepFool is able to compute a smaller perturbation than FGSM while keeping similar successful attack ratios. Carlini and Wagner introduce adversarial attack methods that make quasi-imperceptible perturbations by restricting  $\ell_0$ ,  $\ell_2$  and  $\ell_\infty$  norms. The CW attack not only breaks some of the well accepted adversarial defense methods such as defensive distillation [Papernot *et al.*, 2016a], but also achieves remarkable transferability, in the sense that it can also be used for *black box* attacks when the parameters of a model is unknown.

### 2.2 Adversarial defense

Adversarial defense aims to counter the adversarial effect and to make DNNs achieve performance on adversarial samples close to results on clean samples. Existing approaches can be roughly classified as (1) use of additional denoising structures before the DNN, and (2) enforcing the DNN to become more robust against adversarial attacks.

**Additional denoising structures.** MagNet [Meng and Chen, 2017] is a framework consisting of a detector that rejects adversarial samples that are far away the normal input manifolds and a reformer that finds the closest normal input if the adversarial input is not far from the manifolds. A similar approach is HGD [Liao *et al.*, 2018] which applies high-level representation guided denoiser, so that it can be designed as a defense model that transforms adversarial inputs to easy-to-classify inputs. Defense-GAN [Samangouei *et al.*, 2018] tries to model the distribution of clean images, and it can find a close output to an adversarial image which does not contain the adversarial changes. Denoised smoothing [Salman *et al.*, 2020] prepends a custom-trained denoiser to a DNN and uses randomized smoothing for training the combination which enforces a non-linear Lipschitz property. PixelDefend [Song *et al.*, 2018] approximates the training distribution using a PixelCNN model and purifies images towards higher probability areas of the training distribution. Compared with our method, all these approaches introduce additional network structures which help to remove adversarial noise from inputs at the cost of increasing the number of parameters of the working model. In our experiment, we also empirically show that MAD outperforms MagNet and Denoised smoothing in most of the test cases.

**DNN model Enhancement.** In this category, adversarial training [Madry *et al.*, 2018; Lee *et al.*, 2020] and defensive distillation [Papernot *et al.*, 2016a] are among the early successful approaches. In particular, adversarial training introduces adversarial samples at the training stage to enhance resistance against attacks. Defensive distillation transfers one DNN to another with the same functionality but less sensitive

to input perturbations. However, both adversarial training and defensive distillation require substantially more training cost. Introducing randomized variation to inputs and network parameters at the time of training as been discussed in [Potdevin *et al.*, 2019; Gu and Rigazio, 2015]. Parseval networks [Cisse *et al.*, 2017] limits the Lipschitz constant of linear, convolutional and aggregation layers in the network to be smaller than 1, making these layers tight frames. PCL [Mustafa *et al.*, 2019] separates the hidden feature of different categories by designing a new loss function and bypass network, so as to increase the difficulty of adversarial attacks and achieve the effect of adversarial defense. Since the existing DNN models are already being optimized regarding performance (e.g., neural network search (NAS) [Zoph and Le, 2016] technology is widely used to find neural networks structure with better performance), the modification of DNN structures may introduce human bias, resulting in unpredictable performance degradation. In contrast, our approach MAD does not require any change to network structure or loss function design.

### 3 Mask-based adversarial defense

In this paper we focus on DNNs that classify images. Formally, a DNN is a function  $f_\theta$  which maps  $\mathcal{X} \subseteq \mathbb{R}^d$  to  $\mathcal{Y}$ , where  $\theta$  represents values for the network parameters that are determined at training,  $d$  is the dimension of the input space,  $\mathcal{X}$  is the input space for images and  $\mathcal{Y}$  is a finite set of classes or labels to be returned from  $f_\theta$ . An adversarial input can be written as  $x' = x + \delta$  with  $x$  a clean input and  $\|\delta\|_p < \epsilon$ , such that  $f_\theta(x) \neq f_\theta(x')$ , where  $\|\delta\|_p$  is the  $p$  norm of the perturbation  $\delta$  and  $\epsilon > 0$  is of negligible size, making  $x$  and  $x'$  in the same class to a human being.

#### 3.1 Training a classifier for masked images

A natural approach to counter an adversarial input  $x'$  is to reduce the effect of perturbation  $\delta$ . Given  $\delta$  combined with the pixels of a natural image  $x$ , masking part of  $x'$  would potentially reduce the adversarial effect of  $\delta$ . Fortunately, such a masking operation which “covers” parts of an image does not necessarily make the classification job more difficult for DNNs. Since natural images are heavy in spatial information redundancy, as shown in [He *et al.*, 2021], in which missing pixels of an image can be reconstructed by the state-of-the-art MAE model even though a large amount of input pixels are masked.<sup>1</sup> Since the task of classification is supposed to be easier than reconstruction, this leads us to our first step of training a DNN classifier for masked images, keeping the same network structure as the original DNN to be defended.

Define  $\tau : \mathbb{R}^d \times C \rightarrow \mathbb{R}^d$  a masking operator, where  $C$  is a pre-defined set which has its cardinality depending on the number of grids that cover the input. For example, masking a  $4 \times 4$  image by using  $2 \times 2$  grids gives  $2^4 = 16$  possible ways of masking (2 possibilities for each grid), so that in this case one may set  $|C| = 16$ . (The extreme case is that all grids are masked, but this can hardly happen as we are to explain in our experiment.) Suppose the original classifier  $f_\theta$  is trained with sample set  $Z$ , we use sample set  $Z \times C$  to retrain the

<sup>1</sup>Our human brains possess similar power of recognizing (or even reconstructing) a partially masked object.

# tests	1	3	5	7
precision	75.89%	81.78%	82.65%	82.97%

Table 1: The precision of retrained model for 3/4 masked images from CIFAR-10 with multiple tests

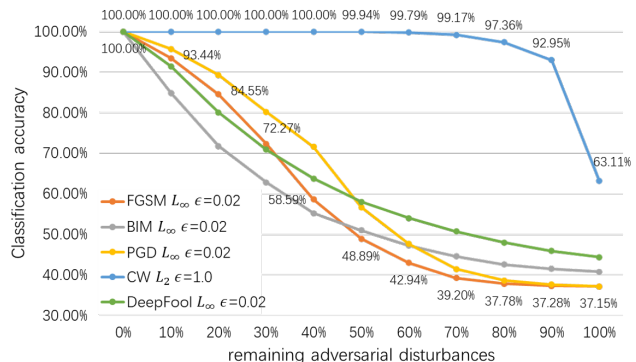


Figure 2: An experiment showing weakened effect of partially removed adversarial vectors generated from CIFAR-10 samples on the accuracy of a VGG16 network.

structure into a new DNN model  $f_{\theta'}$  :  $\mathbb{R}^d \rightarrow \mathcal{Y}$  that is used to “simulate” the performance of  $f_\theta$ , in the sense that given  $x \in \mathcal{X}$ , the output of  $f_{\theta'}(\tau(x, c))$  should approximate  $f_\theta(x)$ , given  $c \in C$  randomly picked.

In the proposed method, images are partially masked in both the training and test phases. For our experiment, in the training phase, each image from the training samples of CIFAR-10 [Krizhevsky and Hinton, 2009] and SVHN [Netzer *et al.*, 2011] is divided into  $8 \times 8$  grids, and images from MNIST [Lecun *et al.*, 1998] are divided into  $7 \times 7$  grids, so that the length of a grid always divides the length of an image (CIFAR-10 and SVHN data sets contain  $32 \times 32$  images and MNIST data set contains  $28 \times 28$  images).

We then conduct a preliminary study on the retrained VGG16 [Simonyan and Zisserman, 2015] classifier for masked images from CIFAR-10, the results shown in Table 1. The original VGG16 model (i.e.,  $f_\theta$ ) has 84.18% accuracy on the test data. The retrained model (i.e.,  $f_{\theta'}$ ) is obtained by letting each  $8 \times 8$  grid have 3/4 probability to be masked, and similarly, test images also have 3/4 probability for each  $4 \times 4$  grid to be masked. Note that in Table 1, “#tests” indicates that we also combine results from multiple tests (i.e., 3, 5, or 7 tests) of the same image with randomized masking applied, and the mostly occurred class of all test results is returned as output for that image. It can be easily seen that applying masking on images with a single test does imply performance degradation (75.89% dropped from 84.18%). However, it seems that the loss of precision can be remedied by applying randomized multiple tests on the same image followed by taking the most favored class, as one may see that in the case of combining 7 tests a precision of 82.97% can be achieved.

#### 3.2 Mitigating adversarial attacks

In our next step, we investigate how the new model trained for masked images can be used to boost defense against ad-

versarial inputs. Given an adversarial input  $x' = x + \delta$ , the new model produces  $f_{\theta'}(\tau(x + \delta, c))$ . Let  $\delta' = \tau(x + \delta, c) - \tau(x, c)$ , which is the actual perturbation on the input to  $f_{\theta'}$ , it is obvious that we have  $\|\delta'\|_p \leq \|\delta\|_p$  for any  $p$ , since only unmasked pixels of  $x$  gets affected by  $\delta$ . As an example, suppose  $3/4$  of the input pixels are masked, the expected  $\ell_1$  norm of  $\delta'$  is only about  $1/4$  in size of the  $\ell_1$  norm of the original perturbation  $\delta$ .

In order to measure how much effect of adversarial inputs is weakened by masking, we conduct another preliminary study by randomly removing part of the perturbation vector  $\delta$  from an adversarial input. We train a VGG16 network on CIFAR-10 data set using the conventional method. Then adversarial samples are generated from clean samples, from which we obtain a perturbation vector by taking the difference between an adversarial input and its corresponding clean image. These vectors are then randomly masked before adding back to the clean images to form a set of weakened attack samples. The relationship between network accuracy and the proportion of the remaining adversarial disturbance is shown in Figure 2, where 100% remaining adversarial disturbance represents strength of the original adversarial inputs, and 20% remaining represents the adversarial inputs with 80% of the perturbation dimensions removed. In particular, we find that the CW attack is more sensitive to this perturbation removal operation, which may be due to that CW generates perturbations with higher relevance. For most other attacks, we find that removing at least 60% of the perturbation (i.e., 40% of the attack remaining) is required to deliver significant improvement regarding classification accuracy.

In general, there is often a trade-off between the strength of defense and the degree of accuracy. As shown in Table 2 of our experiment in the next section, after fixing a network structure, increasing the percentage of covered pixels (at both the training and test phases) often results in a stronger defense against most of the tested adversarial attacks, but with less accurate classification results on benign (clean) inputs. For example, given the first FGSM attack with perturbation degree 15 and mask rate of  $1/3$  yields a model with defense accuracy of 70.17% on adversarial samples, which is less effective compared to the 85.3% accuracy when each grid has a  $4/5$  probability of being masked. However, the  $4/5$ -masked-model only has 76.14% accuracy on benign images, while the  $1/3$ -masked-model has 85.31% accuracy.

## 4 Experiment

The experiments are based on TensorFlow 2.6 and completed on a server running Ubuntu 18.04LTS with a NVIDIA GeForce RTX 3090 GPU. The Adam optimizer is used in training phase with learning rate 0.001. Foolbox [Rauber *et al.*, 2017] is used to generate adversarial samples for the test set. We choose three popular DNN models (LeNet with MNIST [Lecun *et al.*, 1998], VGG16 [Simonyan and Zisserman, 2015] with CIFAR-10 [Krizhevsky and Hinton, 2009] and ResNet18 [He *et al.*, 2016] with SVHN [Netzer *et al.*, 2011]). In order to achieve a classification accuracy close to its corresponding DNN model on benign (clean) images, a MAD model is tested with 20 randomly masked images

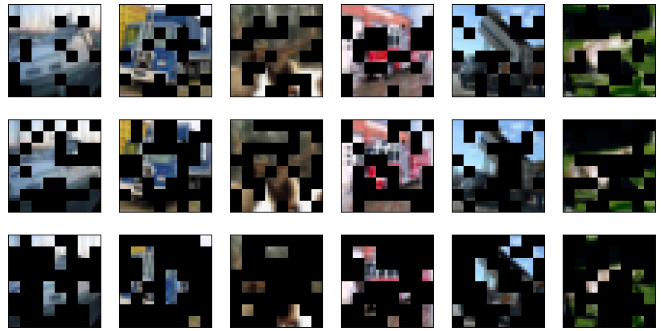


Figure 3: Images from CIFAR-10 with different masking rates applied: from top to bottom,  $1/3$ ,  $1/2$  and  $3/4$  rates are respectively applied on the same images.

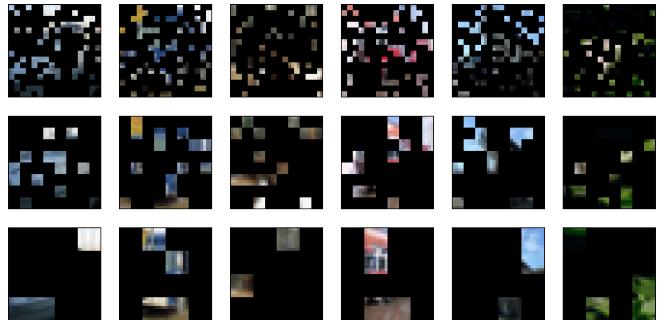


Figure 4:  $3/4$  masked Images from CIFAR-10 with different grid sizes: from top to bottom,  $2 \times 2$ ,  $4 \times 4$  and  $8 \times 8$  grids are used for masking the same images.

transformed from a given image, followed by taking the most favored class of all 20 tests as the output.

**Basic settings for adversarial attack and defense.** We leave the parameters of all adversarial attack methods as default, except for the perturbation degree  $\epsilon$ , which is given along with the ‘‘Attack method’’ in the tables. Note that for all experiments in this paper, adversarial samples are generated only from benign images that are correctly classified by the DNNs to be attacked. The adversarial methods also take into account the parameters of the MAD model (in which sense they are white-box attacks). The generated adversarial samples aim to lower the accuracy of the MAD model without masking being applied, e.g., the FGSM L1 with  $\epsilon = 10$  attack results in a 44.12% accuracy. When multiple randomized masking is applied at testing, the accuracy of the MAD model becomes 68.94% (with 24.82% improvement) facing the same adversarial samples.

**On the mask rate and grid size.** The effectiveness of MAD also depends on two critical hyperparameters. The **mask rate** is a constant which is used as the probability for a grid to be masked at the training phase as well as test phase. As mentioned before, a larger mask rate potentially remove more perturbation (which means better defense) at the cost of less usable information for the classifier, which may lead to worse accuracy on clean images.

We carry out an experiment on a selection of mask rates

Attack method	0	1/3	1/2	3/4	4/5
Benign	<b>84.18%</b>	85.31%	84.59%	82.65%	76.14%
FGSM L1 $\epsilon=15$	63.53%	70.17%	78.37%	82.63%	<b>85.30%</b>
FGSM L1 $\epsilon=20$	63.01%	64.82%	73.70%	79.25%	<b>82.14%</b>
FGSM L2 $\epsilon=0.3$	67.36%	75.95%	82.46%	84.62%	<b>87.55%</b>
FGSM L2 $\epsilon=0.4$	66.23%	70.18%	78.33%	81.89%	<b>84.66%</b>
FGSM Linf $\epsilon=0.01$	48.88%	68.87%	76.07%	81.05%	<b>83.74%</b>
FGSM Linf $\epsilon=0.02$	40.76%	53.77%	61.30%	68.77%	<b>70.61%</b>
BIM L1 $\epsilon=10$	59.02%	67.66%	79.63%	84.71%	<b>87.88%</b>
BIM L1 $\epsilon=15$	58.23%	51.27%	68.89%	80.91%	<b>84.91%</b>
BIM L2 $\epsilon=0.3$	61.86%	61.60%	75.69%	83.21%	<b>87.04%</b>
BIM L2 $\epsilon=0.4$	61.57%	49.33%	68.02%	80.88%	<b>84.25%</b>
BIM Linf $\epsilon=0.01$	38.29%	57.77%	72.21%	81.80%	<b>86.14%</b>
BIM Linf $\epsilon=0.015$	37.15%	39.75%	58.60%	77.06%	<b>82.61%</b>
PGD L1 $\epsilon=15$	58.49%	64.60%	79.17%	85.44%	<b>88.11%</b>
PGD L1 $\epsilon=20$	57.69%	54.85%	73.67%	83.48%	<b>86.89%</b>
PGD L2 $\epsilon=0.3$	62.30%	71.87%	82.82%	86.42%	<b>89.19%</b>
PGD L2 $\epsilon=0.4$	61.63%	62.71%	77.28%	84.45%	<b>87.83%</b>
PGD Linf $\epsilon=0.01$	40.29%	65.37%	77.61%	84.78%	<b>88.26%</b>
PGD Linf $\epsilon=0.015$	37.16%	49.63%	67.64%	81.45%	<b>85.63%</b>
CW L2 $\epsilon=1$	63.11%	95.46%	<b>95.87%</b>	91.28%	93.24%
DeepFool L2 $\epsilon=0.6$	53.97%	74.01%	80.90%	84.20%	<b>87.22%</b>
DeepFool L2 $\epsilon=0.8$	52.61%	68.15%	76.07%	81.19%	<b>83.86%</b>
DeepFool Linf $\epsilon=0.01$	50.70%	75.72%	82.95%	85.23%	<b>87.59%</b>
DeepFool Linf $\epsilon=0.015$	44.32%	67.31%	75.12%	80.44%	<b>83.81%</b>

Table 2: Defense of different mask rates with the grid size of  $8 \times 8$  for the training phase and  $4 \times 4$  for test phase, on a VGG16 model with CIFAR-10 data set

(1/3, 1/2, 3/4, 4/5, sample images illustrated in Figure 3) with grid size fixed at  $8 \times 8$  for the training phase and  $4 \times 4$  for the test phase, on a VGG16 model with image data from CIFAR-10. Note that this only serves as a rough estimate to the optimal rate from the selected list of values, and the final choice is by no means conclusive. Moreover, it is likely that different DNN models have different optimal mask rates that need to be determined each time before the application of MAD. The experimental results are shown in Table 2. It can be seen from the results that higher masking percentage makes better defense but lower accuracy on benign inputs. Considering that in a real life scenario, a DNN may receive a mixed set of benign and adversarial inputs, say 1/2 benign samples and 1/2 adversarial samples, for the mask rate of 3/4 and adversarial samples generated by FGSM with  $\epsilon = 15$ , the real-life defense score can then be calculated as the weighted average  $\frac{1}{2} \times 82.63 + \frac{1}{2} \times 82.65\% = 82.64\%$  as a fair guess in this hypothetical scenario. Therefore, we believe that 3/4 could be a reasonable mask rate which yields acceptable accuracy for both benign and adversarial inputs, and use it for all experiments conducted in rest of the paper.

The **grid size** is another hyperparameter to be determined before the main experiment. Intuitively, a larger grid size allows better continuity of information on average that is preserved in a masked image, examples illustrated in Figure 4. Table 4 presents the preliminary experimental results on a VGG model with CIFAR-10 data set for a selection of grid size values in the masking operation at the time of training and testing, respectively. Given images in CIFAR-10 are of size  $32 \times 32$ , we try a number of combinations for values that divide 32, and again, we do not claim that we are able to find an optimal setting in such an experiment. If we focus on the three columns where  $8 \times 8$  grids are used for training, the results seem to suggest that using a larger grid in the test phase produces a better classification accuracy on benign

	Attack method	Attack	Defense	Improvement	
LeNet + MNIST	Benign		96.13%		
	FGSM L1 $\epsilon=10$	44.12%	68.94%	24.82%	
	FGSM L1 $\epsilon=20$	28.35%	49.50%	21.15%	
	FGSM L2 $\epsilon=0.8$	34.85%	58.60%	23.75%	
	FGSM L2 $\epsilon=1.0$	30.28%	52.82%	22.54%	
	FGSM Linf $\epsilon=0.03$	36.26%	61.82%	25.56%	
	FGSM Linf $\epsilon=0.04$	28.58%	50.31%	21.73%	
	BIM L1 $\epsilon=4$	8.98%	59.49%	50.51%	
	BIM L1 $\epsilon=6$	2.26%	44.17%	41.91%	
	BIM L2 $\epsilon=0.2$	16.55%	69.23%	52.68%	
	BIM L2 $\epsilon=0.3$	3.79%	49.04%	45.25%	
	BIM Linf $\epsilon=0.015$	11.72%	70.94%	59.22%	
	BIM Linf $\epsilon=0.02$	3.62%	56.33%	52.71%	
	PGD L1 $\epsilon=4$	16.04%	71.79%	55.75%	
	PGD L1 $\epsilon=6$	3.37%	54.75%	51.38%	
	PGD L2 $\epsilon=0.2$	22.98%	77.87%	54.89%	
	PGD L2 $\epsilon=0.4$	1.26%	48.85%	47.59%	
	PGD Linf $\epsilon=0.015$	11.64%	70.90%	59.26%	
	PGD Linf $\epsilon=0.02$	3.27%	56.38%	53.11%	
	CW L2 $\epsilon=1.5$	0.20%	93.39%	93.19%	
	DeepFool L2 $\epsilon=0.6$	32.62%	61.05%	28.43%	
	DeepFool L2 $\epsilon=0.8$	26.49%	51.39%	24.90%	
	DeepFool Linf $\epsilon=0.05$	24.77%	47.26%	22.49%	
	DeepFool Linf $\epsilon=0.07$	22.50%	39.76%	17.26%	
	VGG16 + CIFAR-10	Benign		82.65%	
		FGSM L1 $\epsilon=15$	35.48%	82.63%	47.15%
		FGSM L1 $\epsilon=20$	33.02%	79.25%	46.23%
		FGSM L2 $\epsilon=0.3$	38.29%	84.62%	46.33%
		FGSM L2 $\epsilon=0.4$	35.27%	81.89%	46.62%
		FGSM Linf $\epsilon=0.01$	33.02%	81.05%	48.03%
		FGSM Linf $\epsilon=0.02$	28.27%	68.77%	40.50%
		BIM L1 $\epsilon=10$	10.23%	84.71%	74.48%
		BIM L1 $\epsilon=15$	6.70%	80.91%	74.21%
		BIM L2 $\epsilon=0.3$	9.43%	83.21%	73.78%
		BIM L2 $\epsilon=0.4$	8.06%	80.88%	72.82%
BIM Linf $\epsilon=0.01$		3.16%	81.80%	78.64%	
BIM Linf $\epsilon=0.015$		1.06%	77.06%	76.00%	
PGD L1 $\epsilon=15$		8.75%	85.44%	76.69%	
PGD L1 $\epsilon=20$		6.36%	83.48%	77.12%	
PGD L2 $\epsilon=0.3$		12.47%	86.42%	73.95%	
PGD L2 $\epsilon=0.4$		9.01%	84.45%	75.44%	
PGD Linf $\epsilon=0.01$		6.13%	84.78%	78.65%	
PGD Linf $\epsilon=0.015$		2.30%	81.45%	79.15%	
CW L2 $\epsilon=1$		15.89%	91.28%	75.39%	
DeepFool L2 $\epsilon=0.6$		34.64%	84.20%	49.56%	
DeepFool L2 $\epsilon=0.8$		31.81%	81.19%	49.38%	
DeepFool Linf $\epsilon=0.01$		35.72%	85.23%	49.51%	
DeepFool Linf $\epsilon=0.015$		32.26%	80.44%	48.18%	
ResNet18 + SVHN		Benign		91.65%	
		FGSM L1 $\epsilon=15$	50.47%	76.84%	26.37%
		FGSM L1 $\epsilon=20$	45.85%	70.25%	24.40%
		FGSM L2 $\epsilon=0.4$	53.17%	80.40%	27.23%
		FGSM L2 $\epsilon=0.6$	46.77%	71.48%	24.71%
		FGSM Linf $\epsilon=0.01$	57.12%	85.40%	28.28%
		FGSM Linf $\epsilon=0.02$	46.06%	68.95%	22.89%
		BIM L1 $\epsilon=10$	15.46%	80.37%	64.91%
		BIM L1 $\epsilon=12$	11.54%	75.85%	64.31%
		BIM L2 $\epsilon=0.25$	21.75%	84.40%	62.65%
		BIM L2 $\epsilon=0.3$	16.59%	81.37%	64.78%
	BIM Linf $\epsilon=0.01$	16.06%	86.31%	70.25%	
	BIM Linf $\epsilon=0.02$	2.58%	71.00%	68.42%	
	PGD L1 $\epsilon=14$	15.09%	84.14%	69.05%	
	PGD L1 $\epsilon=16$	12.11%	82.35%	70.24%	
	PGD L2 $\epsilon=0.4$	16.40%	84.22%	67.82%	
	PGD L2 $\epsilon=0.5$	12.17%	81.37%	69.20%	
	PGD Linf $\epsilon=0.015$	10.10%	84.45%	74.35%	
	PGD Linf $\epsilon=0.02$	4.69%	80.51%	75.82%	
	CW L2 $\epsilon=1.8$	21.70%	96.05%	74.35%	
	DeepFool L2 $\epsilon=0.5$	59.78%	87.09%	27.31%	
	DeepFool L2 $\epsilon=0.7$	53.87%	82.22%	28.35%	
	DeepFool Linf $\epsilon=0.01$	57.10%	88.06%	30.96%	
	DeepFool Linf $\epsilon=0.02$	46.39%	72.98%	26.59%	

Table 3: Defense against adversarial attacks by MAD

Training	4×4	4×4	8×8	8×8	8×8
Test	2×2	4×4	2×2	4×4	8×8
Benign	73.23%	76.92%	63.11%	82.65%	82.89%
FGSM L1 $\epsilon=15$	86.63%	83.84%	85.34%	82.63%	75.68%
FGSM L1 $\epsilon=20$	83.20%	79.39%	82.74%	79.25%	71.72%
FGSM L2 $\epsilon=0.3$	89.54%	87.13%	86.17%	84.62%	79.84%
FGSM L2 $\epsilon=0.4$	86.63%	83.41%	85.34%	81.89%	75.11%
FGSM Linf $\epsilon=0.01$	86.10%	82.11%	84.42%	81.05%	73.63%
FGSM Linf $\epsilon=0.02$	73.64%	67.07%	73.93%	68.77%	59.87%
BIM L1 $\epsilon=10$	89.21%	85.66%	87.64%	84.71%	75.67%
BIM L1 $\epsilon=15$	84.62%	79.36%	85.61%	80.91%	65.50%
BIM L2 $\epsilon=0.3$	87.52%	83.55%	86.12%	83.21%	71.88%
BIM L2 $\epsilon=0.4$	83.64%	78.06%	85.50%	80.88%	65.82%
BIM Linf $\epsilon=0.01$	86.60%	81.86%	86.47%	81.80%	68.67%
BIM Linf $\epsilon=0.015$	81.26%	72.97%	83.62%	77.06%	56.05%
PGD L1 $\epsilon=15$	88.99%	84.76%	86.64%	85.44%	76.14%
PGD L1 $\epsilon=20$	85.78%	80.08%	86.23%	83.48%	71.13%
PGD L2 $\epsilon=0.3$	90.35%	87.03%	88.07%	86.42%	78.77%
PGD L2 $\epsilon=0.4$	88.01%	83.48%	87.20%	84.45%	74.79%
PGD Linf $\epsilon=0.01$	88.64%	84.05%	86.61%	84.78%	73.89%
PGD Linf $\epsilon=0.015$	84.57%	77.20%	84.46%	81.45%	65.54%
CW L2 $\epsilon=1$	94.78%	95.25%	89.53%	91.28%	93.94%
DeepFool L2 $\epsilon=0.6$	88.54%	87.10%	85.03%	84.20%	80.31%
DeepFool L2 $\epsilon=0.8$	85.73%	82.75%	82.65%	81.19%	75.53%
DeepFool Linf $\epsilon=0.01$	90.33%	88.21%	85.42%	85.23%	80.42%
DeepFool Linf $\epsilon=0.015$	86.03%	82.66%	82.16%	80.44%	74.92%

Table 4: Defense effects of different grid sizes with mask rate of 3/4 on VGG16 and CIFAR-10.

images, and a smaller grid produces a better defense. This time, we choose  $8 \times 8$  (training) and  $4 \times 4$  (testing) for the VGG16 model and CIFAR-10 data set, and adopt this same setting for ResNet and SVHN that also use  $32 \times 32$  images. For the LeNet model and MNIST data set ( $28 \times 28$  images), we use  $7 \times 7$  grids for both training and testing. Likewise, for DNN models not considered in this paper, the grid size to be applied may be different.

## The main result and comparison

The main experiment is conducted on three different models, LeNet with MNIST data set, VGG16 with CIFAR-10, and ResNet18 with SVHN, with the results presented in Table 3. Of all the attacks, CW [Carlini and Wagner, 2017] is the most successfully defended method by MAD. A possible explanation is that CW usually produces highly correlated perturbation, which can be more easily countered by masking as presented in Figure 2. For each attack method with different perturbation degrees ( $\epsilon$ ), MAD tends to achieve a better defense on the attack with a smaller  $\epsilon$ , which is not surprising.

We compare MAD with four state-of-the-art adversarial defence methods, including MagNet [Meng and Chen, 2017], Denoised smoothing [Salman *et al.*, 2020]<sup>2</sup>, Parseval networks [Cisse *et al.*, 2017]<sup>3</sup>, and PCL [Mustafa *et al.*, 2019] on the same backbone VGG16 model with default setting, and all tested with adversarial samples that are generated from CIFAR-10. Note that the adversarial samples used for comparison are generated only from correctly classified benign samples. None of these defense methods uses adversarial samples in the training phase. The results are shown in Table 5.

In order to make the comparison more comprehensive and

<sup>2</sup><https://github.com/microsoft/denoised-smoothing>

<sup>3</sup><https://github.com/mathialo/parsnet>

Attack method	MagNet	Denoised smoothing	Parseval networks	PCL	MAD
Benign	82.32%	77.92%	77.89%	<b>83.47%</b>	82.65%
FGSM L1 $\epsilon=15$	67.41%	81.97%	43.20%	74.94%	<b>82.63%</b>
FGSM L1 $\epsilon=20$	65.68%	76.50%	33.11%	70.53%	<b>79.25%</b>
FGSM L2 $\epsilon=0.3$	72.15%	<b>85.88%</b>	52.41%	79.54%	84.62%
FGSM L2 $\epsilon=0.4$	69.75%	81.70%	42.69%	75.32%	<b>81.89%</b>
FGSM Linf $\epsilon=0.01$	57.81%	<b>82.83%</b>	44.22%	75.56%	81.05%
FGSM Linf $\epsilon=0.02$	44.96%	65.25%	20.75%	62.72%	<b>68.77%</b>
BIM L1 $\epsilon=10$	66.56%	80.11%	45.23%	64.03%	<b>84.71%</b>
BIM L1 $\epsilon=15$	62.63%	68.58%	26.22%	48.03%	<b>80.91%</b>
BIM L2 $\epsilon=0.3$	67.63%	77.36%	38.57%	61.26%	<b>83.21%</b>
BIM L2 $\epsilon=0.4$	65.73%	68.06%	24.96%	48.34%	<b>80.88%</b>
BIM Linf $\epsilon=0.01$	51.34%	75.51%	29.54%	59.83%	<b>81.80%</b>
BIM Linf $\epsilon=0.015$	42.84%	62.41%	13.52%	43.31%	<b>77.06%</b>
PGD L1 $\epsilon=15$	67.08%	79.83%	37.84%	66.63%	<b>85.44%</b>
PGD L1 $\epsilon=20$	64.66%	72.81%	24.64%	53.18%	<b>83.48%</b>
PGD L2 $\epsilon=0.3$	71.98%	84.65%	48.20%	76.08%	<b>86.42%</b>
PGD L2 $\epsilon=0.4$	69.44%	79.17%	35.14%	66.70%	<b>84.45%</b>
PGD Linf $\epsilon=0.01$	56.92%	81.17%	36.89%	72.22%	<b>84.78%</b>
PGD Linf $\epsilon=0.015$	47.79%	70.74%	19.35%	54.74%	<b>81.45%</b>
CW L2 $\epsilon=1$	92.58%	<b>99.74%</b>	43.42%	89.48%	91.28%
DeepFool L2 $\epsilon=0.6$	63.84%	65.04%	34.10%	49.95%	<b>84.20%</b>
DeepFool L2 $\epsilon=0.8$	60.45%	57.97%	44.51%	47.68%	<b>81.19%</b>
DeepFool Linf $\epsilon=0.01$	62.79%	81.43%	30.49%	58.80%	<b>85.23%</b>
DeepFool Linf $\epsilon=0.015$	54.26%	71.68%	9.49%	53.28%	<b>80.44%</b>

Table 5: Comparison of effects of different adversarial defense methods on VGG16 and CIFAR-10.

more convincing, the selected defense methods have inherently different underlying approaches. MagNet and Denoised smoothing apply additional denoising structures to reduce the adversarial perturbations. Parseval network restricts the layers’ Lipschitz constant to be less than 1 during the training. PCL enforces hidden layer features of different classes to be apart as much as possible during the training, which is imposed by adding new branch structures and introducing a new loss function. For our experiment on the comparison, the implementations of Denoised smoothing and PCL are publicly available from their corresponding authors, and the codes for MagNet and Parseval network are available from (third party) Gokul Karthik<sup>4</sup> and standard Python library *parsnet*<sup>5</sup>, respectively.

From the results in Table 5, all methods have an acceptable accuracy on benign inputs. However, regarding the list of tested adversarial attacks, MAD outperforms these state-of-the-art defense approaches in most cases.

## 5 Conclusion

In this paper, we have proposed a new mask-based adversarial defense method called MAD, and have conducted extensive experiments showing that our method provides an effective defense against a variety of adversarial attacks.

Moreover, since the attack algorithms are allowed to have access to the parameters of MAD, our defense seems to provide a way to withstand adaptive white-box attacks, as the randomized masking technique may enforce attackers to consider an attack space of size exponential to the number of grids required to cover the input. We plan to study detailed measurement of this effect on adaptive white-box adversarial attack methods in our future work.

<sup>4</sup><https://github.com/GokulKarthik/MagNet.pytorch>

<sup>5</sup><https://github.com/mathialo/parsnet>

## References

- [Carlini and Wagner, 2017] N. Carlini and D. Wagner. Towards evaluating the robustness of neural networks. *IEEE Symposium on Security and Privacy (SP)*, 2017.
- [Cisse *et al.*, 2017] M. Cisse, P. Bojanowski, E. Grave, Y. Dauphin, and N. Usunier. Parseval networks: Improving robustness to adversarial examples. In *ICML*, pages 854–863, 2017.
- [Cohen *et al.*, 2020] G. Cohen, G. Sapiro, and R. Giryes. Detecting adversarial samples using influence functions and nearest neighbors. In *CVPR*, pages 14441–14450, 2020.
- [Goodfellow *et al.*, 2015] I. J. Goodfellow, J. Shlens, and C. Szegedy. Explaining and harnessing adversarial examples. In *ICLR*, 2015.
- [Gu and Rigazio, 2015] S. Gu and L. Rigazio. Towards deep neural network architectures robust to adversarial examples. In *ICLR Workshop*, 2015.
- [He *et al.*, 2016] K. He, X. Zhang, S. Ren, and J. Sun. Deep residual learning for image recognition. In *CVPR*, pages 770–778, 2016.
- [He *et al.*, 2021] Kaiming He, Xinlei Chen, Saining Xie, Yanghao Li, Piotr Dollár, and Ross Girshick. Masked autoencoders are scalable vision learners. *arXiv preprint arXiv:2111.06377*, 2021.
- [Krizhevsky and Hinton, 2009] A. Krizhevsky and G. Hinton. Learning multiple layers of features from tiny images. Technical report, University of Toronto, 2009.
- [Kurakin *et al.*, 2017] A. Kurakin, I. Goodfellow, and S. Bengio. Adversarial examples in the physical world. *ICLR workshop*, 2017.
- [Lecun *et al.*, 1998] Y. Lecun, L. Bottou, Y. Bengio, and P. Haffner. Gradient-based learning applied to document recognition. *Proceedings of the IEEE*, 86(11):2278–2324, 1998.
- [Lee *et al.*, 2020] S. Lee, H. Lee, and S. Yoon. Adversarial vertex mixup: Toward better adversarially robust generalization. In *CVPR*, pages 269–278, 2020.
- [Liao *et al.*, 2018] F. Liao, M. Liang, Y. Dong, T. Pang, X. Hu, and J. Zhu. Defense against adversarial attacks using high-level representation guided denoiser. In *CVPR*, pages 1778–1787, 2018.
- [Ma *et al.*, 2018] X. Ma, B. Li, Y. Wang, M. S. Erfani, N. R. S. Wijewickrema, E. M. Houle, G. Schoenebeck, D. Song, and J. Bailey. Characterizing adversarial subspaces using local intrinsic dimensionality. In *ICLR*, 2018.
- [Madry *et al.*, 2018] A. Madry, A. Makelov, L. Schmidt, D. Tsipras, and A. Vladu. Towards deep learning models resistant to adversarial attacks. In *ICLR*, 2018.
- [Meng and Chen, 2017] D. Meng and H. Chen. Magnet: a two-pronged defense against adversarial examples. In *CCS*, pages 135–147, 2017.
- [Moosavi-Dezfooli *et al.*, 2016] S. Moosavi-Dezfooli, A. Fawzi, and P. Frossard. DeepFool: a simple and accurate method to fool deep neural networks. In *CVPR*, pages 2574–2582, 2016.
- [Mustafa *et al.*, 2019] A. Mustafa, S. Khan, M. Hayat, R. Goecke, J. Shen, and L. Shao. Adversarial defense by restricting the hidden space of deep neural networks. In *ICCV*, pages 3385–3394, 2019.
- [Netzer *et al.*, 2011] Y. Netzer, T. Wang, A. Coates, A. Bischoff, B. Wu, and A. Ng. Reading digits in natural images with unsupervised feature learning. In *NIPS Workshop on Deep Learning and Unsupervised Feature Learning*, 2011.
- [Papernot *et al.*, 2016a] N. Papernot, P. McDaniel, S. Jha, M. Fredrikson, Z. B. Celik, and A. Swami. The limitations of deep learning in adversarial settings. In *IEEE European Symposium on Security and Privacy*, 2016.
- [Papernot *et al.*, 2016b] N. Papernot, P. D. McDaniel, X. Wu, S. Jha, and A. Swami. Distillation as a defense to adversarial perturbations against deep neural networks. In *IEEE Symposium on Security and Privacy (SP)*, pages 582–597. IEEE Computer Society, 2016.
- [Potdevin *et al.*, 2019] Y. Potdevin, D. Nowotka, and V. Ganesh. An empirical investigation of randomized defenses against adversarial attacks. *CoRR*, abs/1909.05580, 2019.
- [Rauber *et al.*, 2017] Jonas Rauber, Wieland Brendel, and Matthias Bethge. Foolbox: A python toolbox to benchmark the robustness of machine learning models. In *Reliable Machine Learning in the Wild Workshop, 34th International Conference on Machine Learning*, 2017.
- [Report, 2020] Report. Neural network market to reach \$38.71 billion, globally, by 2023, says Allied Market Research, 02 April 2020. accessed 29 Dec. 2021.
- [Salman *et al.*, 2020] H. Salman, M. Sun, G. Yang, A. Kapoor, and J. Z. Kolter. Denoised smoothing: A provable defense for pretrained classifiers. In *NeurIPS 2020*. ACM, 2020.
- [Samangouei *et al.*, 2018] Pouya Samangouei, Maya Kabkab, and Rama Chellappa. Defense-GAN: protecting classifiers against adversarial attacks using generative models. *arXiv preprint arXiv:1805.06605*, 2018.
- [Simonyan and Zisserman, 2015] K. Simonyan and A. Zisserman. Very deep convolutional networks for large-scale image recognition. In *ICLR*, 2015.
- [Song *et al.*, 2018] Y. Song, T. Kim, S. Nowozin, S. Ermon, and N. Kushman. Pixeldefend: Leveraging generative models to understand and defend against adversarial examples. In *ICLR*, 2018.
- [Szegedy *et al.*, 2014] C. Szegedy, W. Zaremba, I. Sutskever, J. Bruna, D. Erhan, I. Goodfellow, and R. Fergus. Intriguing properties of neural networks. In *ICLR*, 2014.
- [Xu *et al.*, 2018] W. Xu, D. Evans, and Y. Qi. Feature squeezing: Detecting adversarial examples in deep neural networks. In *NDSS*, 2018.
- [Zoph and Le, 2016] Barret Zoph and Quoc V Le. Neural architecture search with reinforcement learning. *arXiv preprint arXiv:1611.01578*, 2016.